Surface Organometallic Chemistry on Metals: Formation of a Stable ≡Sn(n-C_4H_9) Fragment as a Precursor of Surface Alloy Obtained by Stepwise Hydrogenolysis of Sn(n-C_4H_9)$_4$ on a Platinum Particle Supported on Silica

F. Humblot,[†] D. Didillon,[‡] F. Lepeltier,[‡] J. P. Candy,*[,†] J. Corker,[§] O. Clause,[‡] F. Bayard,[†] and J. M. Basset*[,†]

Contribution from the Laboratoire de Chimie Organométallique de surface, UMR CNRS-CPE 9986, CPE, 43 Bd du 11 novembre 1918, 69100 Villeurbanne, France, Institut Français du Pétrole, 1 et 4 Avenue de bois-Préau, 92506 Rueil-Malmaison Cédex, France, and Department of Chemistry, University of Southampton, Southampton 509 5NH, U.K.

Received December 23, 1996. Revised Manuscript Received August 18, 1997[⊗]

Abstract: Selective hydrogenolysis of Sn(n-C_4H_9)$_4$ on a Pt/SiO_2 catalyst has been carried out at various temperatures and coverages of the metallic surface to prepare via surface organometallic chemistry a well-defined class of bimetallic catalysts. The stoichiometry and kinetics of the reaction was followed by the careful analysis of reagents and products, including extraction of unreacted reagents, and elemental analysis of the samples. The various surface species formed were characterized by electron microscopy (CTEM and TEM EDAX) and EXAFS analysis. Possible structures of the surface organometallic fragments were considered using molecular modeling. At 50 °C, the hydrogenolysis reaction occurs selectively on the platinum surface with exclusive evolution of *n*-butane. There is first formation of a Sn(n-C_4H_9)$_3$ fragment grafted on the platinum particle which undergoes a stepwise cleavage of two tin−carbon σ-bonds to form a stable Pt−Sn(n-C_4H_9) fragment. Regardless of the reaction time, surface coverage, or loading, the number of grafted butyl fragments per platinum is never greater than unity, that is to say that when Sn(n-C_4H_9)$_3$ is formed the platinum coverage by tin is 0.3 whereas when Sn(n-C_4H_9) is formed the platinum coverage is closer to 1. It is therefore suggested that the surface composition is governed by the bulkiness of the *alkyl chains* which are "close packed" on the surface. At 100 °C, the reaction takes place both on the platinum and the silica surface. On the platinum surface, the same fragments (namely Sn(n-C_4H_9)$_3$, Sn(n-C_4H_9)$_2$, and Sn(n-C_4H_9)) were identified, but simultaneously on the silica surface, the well-described ≡SiOSn(n-C_4H_9)$_3$ species was also formed. Thermal treatment under hydrogen of Pt$_s$−Sn(n-C_4H_9) lead to alkyl-free tin atoms which are located at the periphery of the particle as evidenced by Sn K edge EXAFS (Pt−Sn distance of 2.75 Å with a coordination number of ca. 4). Even if the organotin fragments are grafted with a coverage of unity, after their complete hydrogenolysis at 300 °C, about 40% of the platinum is still accessible to H_2 chemisorption. This could be explained by the increase of the particle diameter (+0.5 Å) which prevents a close packing of the tin atoms around the particle and leaves some platinum atoms still accessible to the hydrogen. After treatment of the catalyst at higher temperatures, typically 500 °C, the structure of the catalyst is slightly changed since the tin atoms migrate into the first monolayer of the particle, as evidenced by a significant increase of the tin coordination number (ca. 4.4−5.6) as determined by EXAFS. Hypothetical surface structures have been proposed on the basis of molecular modeling of platinum particles covered by various surface organotin fragments.

1. Introduction

Platinum−tin bimetallic catalysts are widely used in petrochemistry for example in reforming or in isobutane dehydrogenation.[1−10] It has been recently shown that surface organometallic chemistry on metal can be a clean and controlled route for the preparation of bimetallic materials.[11] For example, the controlled hydrogenolysis reaction of tetra-*n*-butyltin (Sn(n-C_4H_9)$_4$) with the surface of group VIII metals leads to bimetallic catalysts which exhibit very high selectivities and activities in the hydrogenolysis of ethyl acetate into ethanol,[12] hydrogenation

[†] UMR CNRS-CPE 9986.
[‡] Institut Français du Pétrole.
[§] University of Southampton.
[⊗] Abstract published in *Advance ACS Abstracts,* December 15, 1997.

(1) Loc, L. C.; Gaidai, N. A.; Kiperman, S. L. *Proc. Int. Congr. Catal., 9th* **1988**, *3*, 1261.
(2) Barias, O. A.; Holmen, A.; Blekkan, E. A. *Stud. Surf. Sci. Catal.* **1994**, *88*, 519.
(3) Cortright, R. D.; Dumesic, J. A. *J. Catal.* **1994**, *148*, 771.
(4) Yarusov, I. B.; Zatolokina, E. V.; Shitova, N. V.; Belyi, A. S.; Ostrovski, N. M. *Catal. Today* **1992**, *13*, 655.
(5) Wilhelm, F. Dutch Patent 2 164 295, 1972.
(6) Wang, L.; Lin, L.; Zang, T.; Cai, H. *React. Kinet. Catal. Lett.* **1994**, *52*, 107.
(7) Muller, A. C.; Engelhard, P. A.; Weisang, J. E. *J. Catal.* **1979**, *56*, 65.
(8) Coq, B.; Figuéras, F. *J. Catal.* **1984**, *85*, 197.
(9) Carter, J. L.; McVicker, G. B.; Weissman, W.; Kmak, W. S.; Sinfelt, J. H. *Appl. Catal.* **1982**, *3*, 327.
(10) Burch, R.; Garla, L. A. *J. Catal.* **1981**, *71*, 360.
(11) Candy, J. P.; Didillon, B. D.; Smith, E. L.; Shay, T. B.; Basset, J. M. *J. Mol. Catal.* **1994**, *86*, 179.

S0002-7863(96)04405-8 CCC: $15.00
Published on Web 01/14/1998

of nitrobenzene into aniline,[13] hydrogenation of α−β unsaturated aldehyde into the corresponding unsaturated alcohol,[14−16] and ethylene hydroformylation into propanal or propanol.[17] These high selectivities are ascribed to relatively well defined new catalytic materials which can be divided in three categories in the case of the Rh−Sn, Ru−Sn, and Ni−Sn systems:

(1) The organometallic fragment is still coordinated to the metal and plays the role of a ligand as in classical molecular catalysis.

(2) The surface organometallic fragment is decomposed into "adatoms" which are presumably formed selectively on some crystallographic positions of the particule; the role of these adatoms is that of a selective poison, a well-known concept in heterogeneous catalysis.

(3) The organometallic fragment is fully hydrogenolized, and the tin atoms are incorporated into the metallic lattice in a regular manner leading to site isolation effects.

Most of the preceeding studies concern Rh,[18−26] Ru,[23] Ni,[23,27,28] and Pt.[29−33] In the family of group VIII metals, the platinum−tin combination is by far the most important class of bimetallic catalysts due to their role in reforming. Their preparation is usually achieved by a procedure of impregnation and reduction. However, such a mode of preparation does not always lead to very reproducible results. To precisely control the preparation of the bimetallic Pt−Sn material, the use of organometallic precursors which are selectively chemisorbed on the metallic particles seems to be a promising, elegant, and very useful procedure. However, it is necessary to understand the complete reaction pathway during the hydrogenolysis of $Sn(n\text{-}C_4H_9)_4$ with the reduced Pt surface. Generally, this reaction is performed in *n*-heptane[34] or in benzene solution,[33] but the presence of a solvent makes it very difficult to characterize the intermediate complexes formed. This article reports the study of the hydrogenolysis of $Sn(n\text{-}C_4H_9)_4$ without any solvent on a silica-supported platinum surface and the characterization of the various surface species at all the stages of their preparation.

2. Experimental Section

2.1. Monometallic Silica-Supported Platinum Catalyst. The preparation of the monometallic catalyst has been described elsewhere.[35] The silica support Aerosil 200 $m^2\ g^{-1}$ was purchased from Degussa. The platinum salt, $Pt(NH_3)_4(OH)_2$, was purchased from STREM Chem. Inc. The platinum complex is grafted onto the silica surface by the reaction of $Pt(NH_3)_4(OH)_2$ with the Si OH groups of the silica surface. This ionic exchange is achieved by stirring the slurry of the silica and the platinum salt for 10 h. After filtration, the surface complex obtained is decomposed by calcination under a mixture of nitrogen/oxygen (5/1) at increasing temperatures from 25 to 400 °C (1 °C·min^{-1}). The solid obtained is reduced under flowing hydrogen at 400 °C for 4 h and then stored at room temperature in air. Analysis of the platinum and tin in the samples was achieved after treatment with HNO_3 + HCl and then HF. After dissolution of the solid, quantitative analysis was carried out by atomic absorption.

2.2. Chemisorption Measurements. Gas adsorption measurements were carried out at room temperature using conventional Pyrex volumetric adsorption equipment.[36] The vacuum (10^{-6} mbar) was achieved with a liquid nitrogen trapped mercury diffusion pump. The equilibrium pressure was measured with a Texas Instrument gauge (pressure range 0−1000 mbar with an accuracy of 0.1 mbar). The catalyst sample was placed in a Pyrex flow-through cell to enable reduction in flowing hydrogen at 773 K. After reduction, the cell was sealed and the sample was outgassed at 530 °C for 2 h under vacuum before gas chemisorption measurements.

2.3. Hydrogenolysis of $Sn(n\text{-}C_4H_9)_4$ on Silica Support and on Reduced Pt Particles. This reaction was performed in the same apparatus as described above. After reduction under flowing H_2, the sample (silica or silica-supported platinum) was sealed under H_2 and then kept at room temperature under 30 mbar of H_2. The desired amount of $Sn(n\text{-}C_4H_9)_4$ was then carefully introduced into the reactor via a septum to avoid contact with air. The reaction was performed at two temperatures: 50 and 100 °C. The gases evolved during the reaction were trapped at 77 K (liquid nitrogen temperature) elsewhere in the apparatus, to avoid possible feedback of the gases onto the catalytic surface and further hydrogenolysis. After various times of reaction, the reactor was isolated and the temperature of the cold part was raised to room temperature. The gases evolved were qualitatively and quantitatively analyzed by GC and volumetric measurements. The liquid nitrogen trap was reestablished and the reaction continued. At the end of the reaction, the solid was washed with *n*-heptane and the amount of unreacted $Sn(n\text{-}C_4H_9)_4$ was measured by GC. The sample was then dried in an oven, and the amount of tin fixed was determined by elemental analysis.

2.4. Electron Microscopy (CTEM and STEM-EDAX). Conventional transmission electron microscopy (CTEM) was performed using JEOL 100 CX electron microscope to establish particle size distributions. Metallic particles were assumed to have cubo-oactahedral shape.[37−39] The surface of such a particle is composed of [111] and [100] faces, and the number of metal atoms on each edges (*m*) is the same. According to Van Hardeveld and Hartog,[40] the diameter of these

(12) El Mansour, A.; Candy, J. P.; Bournonville, J. P.; Ferretti, O. A.; Basset, J. M. *Angew. Chem., Int. Ed. Engl.* **1989**, *28*, 347.
(13) Didillon, B.; Le Peltier, F.; Candy, J. P.; Sarrazin, P.; Boitiaux, J. P.; Basset, J. M. Brevet Français 91.00132, 1991.
(14) Didillon, B.; El Mansour, A.; Candy, J. P.; Basset, J. M.; Le Peltier, F.; Bournonville, J. P. *New organometallic active sites obtained by controlled surface reaction of organometallic complex with supported metal particles;* Poncelet, G., Jacobs, P. A., Grange, P., and Delmon, B., Eds.; Elsevier Science Publishers: Amsterdam, 1991, Vol. 63, p 717.
(15) Didillon, B.; Candy, J. P.; El Mansour, A.; Houtman, C.; Basset, J. M. *J. Mol. Catal.* **1992**, *74*, 43.
(16) Didillon, B.; El Mansour, A.; Candy, J. P.; Basset, J. M.; Le peltier, F.; Boitiaux, J. P. *Proc. Int. Congr. Catal., 10th* **1993**, *75*, 2370.
(17) Izumi, Y.; Asakura, K.; Iwasawa, Y. *J. Catal.* **1991**, *127*, 631.
(18) Tomishige, K.; Asakura, K.; Iwasawa, Y. *J. Chem. Soc., Chem. Commun.* **1993**, 184.
(19) Tomishige, K.; Asakura, K.; Iwasawa, Y. *Catal. Lett.* **1993**, *20*, 15.
(20) Tomishige, K.; Asakura, K.; Iwasawa, Y. *J. Catal.* **1994**, *149*, 70.
(21) Tomishige, K.; Asakura, K.; Iwasawa, Y. *Chem. Lett.* **1994**, 235.
(22) Tomishige, K.; Asakura, K.; Iwasawa, Y. *J. Catal.* **1995**, *157*, 472.
(23) Agnelli, M.; Louessard, P.; El Mansour, A.; Candy, J. P.; Bournonville, J. P.; Basset, J. M. *Catal. Today* **1989**, *6*, 63.
(24) Candy, J. P.; Ferretti, O. A.; Mabilon, G.; Bournonville, J. P.; El Mansour, A.; Basset, J. M.; Martino, G. *J. Catal.* **1988**, *112*, 210.
(25) Candy, J. P.; Ferretti, O. A.; El Mansour, A.; Mabilon, G.; Bournonville, J. P.; Basset, J. M.; Martino, G. *J. Catal.* **1988**, *112*, 210.
(26) Candy, J. P.; El Mansour, A.; Ferretti, O. A.; Mabilon, G.; Bournonville, J. P.; Basset, J. M.; Martino, G. *J. Catal.* **1988**, *112*, 201.
(27) Lesage, P.; Clause, O.; Moral, P.; Didillon, B.; Candy, J. P.; Basset, J. M. *J. Catal.* **1995**, *155*, 238.
(28) Agnelli, M.; Candy, J. P.; Basset, J. M.; Bournonville, J. P.; Ferretti, O. A. *J. Catal.* **1990**, *121*, 236.
(29) Inoue, T.; Tomishige, K.; Iwasawa, Y. *J. Chem. Soc., Chem. Commun.* **1995**, 329.
(30) Inoue, T.; Tomishige, K.; Iwasawa, Y. *J. Chem. Soc., Faraday Trans.* **1996**, *92*, 461.
(31) Margitfalvi, J.; Hegedüs, M.; Talas, E. *J. Mol. Catal.* **1989**, *51*, 279.
(32) Margitfalvi, J.; Göbölös, S.; Talas, E.; Hegedüs, M.; Szedlacsek, P. *Studies in Surface Science Catalysis: Catalyst Deactivation*; Delmon, B., Froment, G. F., Eds.; Elsevier Science Publishers: Amsterdam, 1987, p 147.
(33) Vértes, C.; Talas, E.; Czako, I.; Göbölös, S.; Vértes, A.; Margitfalvi, J. *Appl. Catal.* **1991**, *68*, 149.
(34) Coq, B.; Chaqroune, A.; Figuéras, F.; Nciri, B. *Appl. Catal.* **1992**, *82*, 231.
(35) Benesi, A. H.; Curtis, R. M.; Stude, H. P. *J. Catal.* **1968**, *10*, 328.
(36) Candy, J. P.; Fouilloux, P.; Renouprez, A. J. *J. Chem. Soc., Faraday Trans. 1* **1980**, *76*, 616.
(37) Moraweck, B.; Clugnet, G.; Renouprez, A. *Surf. Sci.* **1979**, *81*, L631.
(38) Yacaman, M. J.; Domingez, E. *Surf. Sci.* **1979**, *87*, L263.
(39) Da Silva, P. N.; Gunier, M.; Leclercq, C.; Frety, R. *Appl. Catal.* **1989**, *54*, 203.
(40) Van Hardeleld, R.; Hartog, F. *Surf. Sci.* **1969**, *15*, 189.

Table 1. Cubo-octahedron Particule of Platinum and Variation of Diameter and Dispersion with the Number *m* of Platinum Atoms on One Edge

no. of atoms on edge (*m*)	no. of total atoms	no. of surface atoms	dispersion	diameter (nm)
2	38	32	0.84	1.03
3	201	122	0.61	1.8
4	586	272	0.46	2.6
5	1289	482	0.37	3.3
6	2406	752	0.31	4.1
8	6266	1472	0.23	5.7
10	12934	2432	0.19	7.2
12	23178	3632	0.16	8.8
14	37766	5072	0.13	10.3

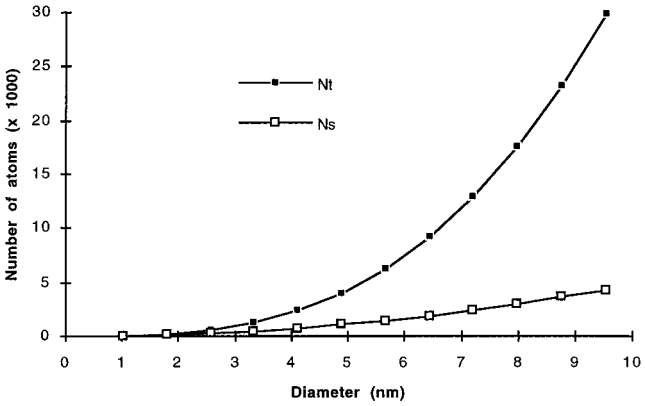

Figure 1. Number of surface atoms (N_s) and number of total atoms (N_t) in function of a cubo-octahedral shape particle diameter.

particles (d_{part}) is given by

$$d_{part} = 1.105 d_{atomic}(N_t)^{1/3} \quad \text{(for platinum, } d_{atomic} = 0.278 \text{ nm)}$$

The number of surface metal atoms (N_s) and the total number of metal atoms (N_t) can be related to the number of metal atom located on one edge (m). The results are reported in Table 1 and Figure 1.

From the CTEM analysis, it is possible to know the amount (n_d) of particles with a given diameter (d), and from the Figure 1, we can deduce the number N_s and N_t for each particle with this diameter (d). From the complete histogram, one may calculate the number of surface atoms ($\sum n_d N_s$) and of total metal atoms ($\sum n_d N_t$). The dispersion of the metallic particle is thus given by $D = \sum n_d N_s / \sum n_d N_t$.

2.5. Extended X-ray Adsorption Fine Structure (EXAFS). The EXAFS measurements were performed at the LURE synchrotron radiation facility using the X-ray beam emitted by the DCI storage ring (positron energy of 1.85 eV and average ring current of ca. 300 mA). Powdered samples for EXAFS analysis were prepared as described above under the strict exclusion of air. EXAFS cells (ca. 0.5−1.0 cm thick) fitted with Kapton windows were built onto break-seal Pyrex tubes containing the silica-supported Pt−Sn samples and evacuated to ca. 0.01 Pa before sample transfer under argon. X-ray absorption spectra were acquired in transmission mode at room temperature using a Si(311) double-crystal monochromator and two Ar-filled ionization chambers as detectors. Edge jumps ranged between 0.5 and 1.0 eV and the total absorption beyond the Sn K-edge between 2 and 2.5 eV. Spectra were accumulated using 3 eV steps starting from 100 eV below the edge to 800 eV above the edge. The DE/E resolution was estimated to 4×10^{-4}. Background-substracted EXAFS data were obtained using the program PAXAS.[41] A polynomial of order 2 was used in the pre-edge background substraction, and the post-edge background was substracted using couple polynomials of order 8 to remove low-frequency contributions from the spectrum. Spherical wave curve fitting analyses, by least-squares refinement of non-Fourier-filtered EXAFS, were carried out in EXCURVE,[42,43] using Von-Barth ground state potentials and Hedin−Lundqvist exchange potentials. Fits were optimized by considering both k^1 and k^3 weighting of the EXAFS since the latter emphasizes the higher shells whereas the former favors near shells of light scatterers. No significant differences were observed for refinements carried out using the two weightings. Selective Fourier filtering of the EXAFS was used to help in the identification of the backscatterers giving rise to peaks occurring in the Fourier transform. The accuracy of bonded and nonbonded interatomic distances is considered to be 1.4% and 1.6%, respectively.[44] Precision on first-shell coordination numbers is estimated to be ca. 5−10% and, for nonbonded shells, between 10 and 20%. The statistical validity of shells was assessed by published means,[45] and the numbers of independent parameters used in the fits fall within the guideline $N_{pts} = 2(k_{max} - k_{min})(R_{max} - R_{min})/\pi$.[46]

(41) Binsted, N. PAXAS Programme for the analysis of X-ray absorption spectra, University of Southampton, 1988.

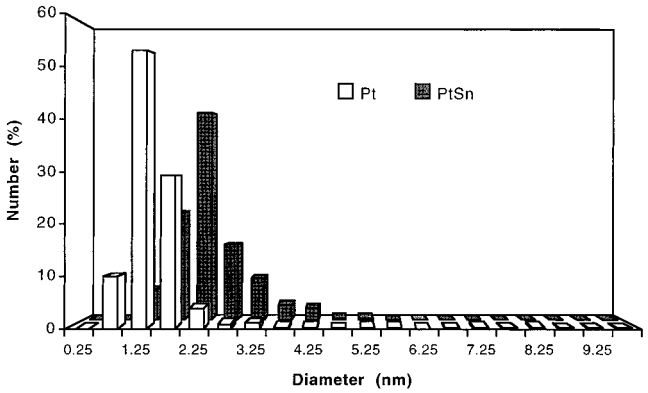

Figure 2. Particle size distribution of Pt/SiO_2 catalyst.

2.6. Molecular Modeling. Metallic particles size was modeled assuming a cubo-octahedral shape. Steric hindrance for Sn complexes grafted on the metallic surface was calculated by using SYBYL molecular modeling software from TRIPOS[47] and Silicon Graphics Indigo as hardware. We used the classical TRIPOS force field data for H and C. Bond distances, angles, and constants not found in the TRIPOS force field were based on the literature values.[48]

3. Results and Discussion

3.1. Characterization of the Monometallic Silica-Supported Platinum Catalyst. Pt/SiO_2 catalyst (1.57%) was prepared according to a classical method of exchange and reduction (see the Experimental Section). The particle size distribution of this Pt/SiO_2 catalyst has been determined by CTEM analysis. A typical histogram is given on Figure 2. The distribution (in surface) is rather narrow with an average particle diameter close to 1.5 nm, but some larger particles (3 nm < d < 10 nm) are detected. The average dispersion of the metallic particles (D), see the Experimental Section, is close to 0.34.

Chemisorption of H_2 and O_2 was used as an indirect method to determine metal particle size. The isotherms of chemisorption for H_2 and O_2 were measured at 25 °C under hydrogen pressures ranging from 0 to 200 mbar. Blank experiments performed in the same condition with the pure silica indicate that the amount of hydrogen adsorbed is negligible, but the amount of oxygen adsorbed increases slightly with the equilibrium pressure to reach ca. 2 μmol/g at 150 mbar. We thus corrected the measured values obtained for oxygen adsorption on the Pt/SiO_2 sample.

(42) Gurman, S. J.; Binsted, N.; Ross, J. *J. Phys. Chem.* **1986**, *19*, 1845.
(43) Gurman, S. J.; Binsted, N.; Ross, J. *J. Phys. Chem.* **1984**, *17*, 143.
(44) Corker, J.; Evans, J. *J. Chem. Soc., Chem. Commun.* **1994**, 1027.
(45) Joyner, R. W.; Martin, K. J.; Meehan, P. *J. Phys. Chem.* **1987**, 4005.
(46) Lytle, F. W.; Sayers, D. E.; Stern, E. A. *Physica B* **1989**, *158*, 701.
(47) TRIPOS: Tripos Associates, 1699 S. Hanley Road, Suite 303, St. Louis, MO 63144.
(48) Allinger, N. L.; Quinn, M. I.; Chen, K.; Thomson, B.; Frierson, M. R. *J. Mol. Struct.* **1989**, *194*, 1.

Table 2. Reaction of Tetrabutyltin with SiO_2 and Pt/SiO_2 (1 g) at 50 and 100 °C and Amount of Tin Fixed and Butane Evolved after 50 h of Reaction

	SiO_2	SiO_2	Pt/SiO_2	Pt/SiO_2
temp (°C)	50	100	50	100
$SnBu_{4\ introduced}$ (μmol/g)	30	63	53.6	49.6
$Sn_{introduced}/Pts$			1.9	1.8
$SnBu_{4\ extracted}$ (μmol/g)	28.2	15	25.4	0
Sn_{fixed}	1.8	48	28	49.6
Sn_{fixed}/Pts			1.0	1.8
C_4/Sn_{fixed}	1	0.9	3	2.4

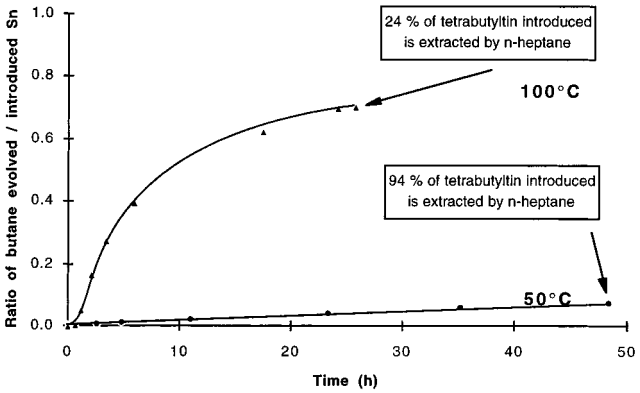

Figure 3. Amount of butane evolved during the reaction of Sn(*n*-$C_4H_9)_4$ on silica at 50 and 100 °C.

There is a plateau for isotherms of chemisorption of hydrogen or oxygen for pressures higher than ca. 50 mbar. At 150 mbar, the amounts of hydrogen and oxygen adsorbed are respectively 25 and 14 μmol/g. If the stoichiometries of 1.8 H/Pt_s and 1 O/Pt_s were assumed for an equilibrium pressure of 150 mbar,[36,49] the number of surface platinum atoms is equal to 28 μmol/g in the two cases. The resulting dispersion (0.35) is consistent with the value obtained from CTEM analysis (0.34).

3.2. Hydrogenolysis of Sn(*n*-$C_4H_9)_4$ on SiO_2 and Pt_s-H_x/SiO_2. 3.2.1. Stoichiometry of the Reaction. The hydrogenolysis reaction of Sn(*n*-$C_4H_9)_4$, under 30 mbar of hydrogen on SiO_2 and Pt_s-H_x/SiO_2, was studied at 50 and 100 °C. For both systems, butane was the only gas evolved. The results are reported in Table 2 and Figure 3.

When the hydrogenolysis reaction is performed at 50 °C on dehydroxylated silica, even after 50 h of reaction, the amount of Sn(*n*-$C_4H_9)_4$ chemically grafted on the silica is very low: 94% of the tetrabutyltin introduced can be extracted intact by *n*-heptane after 50 h of reaction. When the reaction is performed at 100 °C (Table 2) the chemical grafting is not negligible: 24% of tetrabutyltin introduced is extracted by *n*-heptane after 25 h of reaction showing a slow but nevertheless significant reaction with the oxide surface. Note that the induction period observed is due to the time required to reach 100 °C.

The amount of butane evolved corresponds respectively to 0.9 and 1.0 C_4H_{10} per Sn(*n*-$C_4H_9)_4$ fixed for reactions carried out at 50 or 100 °C with the silica. This result is in complete agreement with the formation of the well-defined ≡SiO-Sn(*n*-$C_4H_9)_3$ species,[50] following eq 1. At 50 °C, with Pt_s-H_x/

$$\equiv SiO-H + Sn(n\text{-}C_4H_9)_4 \rightarrow \equiv SiO-Sn(n\text{-}C_4H_9)_3 + n\text{-}C_4H_{10} \quad (1)$$

$SiO_{2(400)}$, the amount of butane evolved with time and for various amounts of Sn(*n*-$C_4H_9)_4$ introduced is much larger than with $silica_{(400)}$ (compare the values of *n*-butane released in Figures 3 and 4). The amount of Sn(*n*-$C_4H_9)_4$ fixed after 50 h of reaction at 50 °C and the corresponding amount of *n*-butane evolved are reported in Table 2. The amount of Sn(*n*-$C_4H_9)_4$ fixed is never greater than 1 Sn/Pt_s, even when the amount of Sn(*n*-$C_4H_9)_4$ introduced corresponds to 1.9 Sn/Pt_s (Table 2). At this temperature, Sn(*n*-$C_4H_9)_4$ reacts with SiO_2 to a very small extent (Table 2, Figure 3), These results suggest that the reaction occurs quite selectively on the metallic surface. However, the hydrogenolysis of Sn(*n*-$C_4H_9)_4$ is never complete, as can be seen in Figure 4 and Table 2: the new organometallic material obtained can be described by the general formula $Pt_s[Sn(n\text{-}C_4H_9)_x]_y$ with $0 < y < 1$.

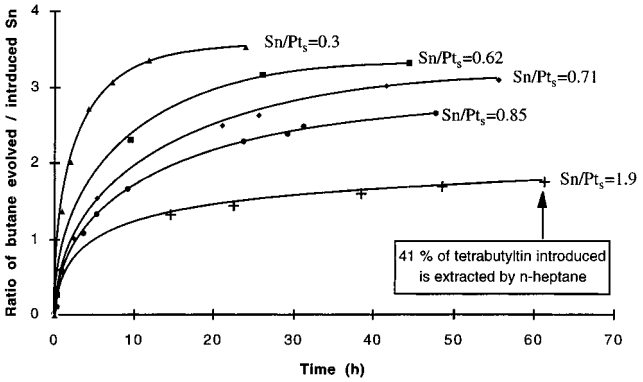

Figure 4. Amount of butane evolved during the reaction of Sn(*n*-$C_4H_9)_4$ on silica-supported platinum at 50 °C for various amounts of Sn(*n*-$C_4H_9)_4$ introduced.

The reaction can be described by the following equation:

$$Pt_s-H + y\,Sn(n\text{-}C_4H_9)_4 \xrightarrow{H_2} Pt_s-[Sn(n\text{-}C_4H_9)_x]_y + y(4-x)\,n\text{-}C_4H_{10} \quad (2)$$

The determination of the mechanism of the hydrogenolysis of the tin alkyl complex is a rather difficult problem to solve. A series of experiments was performed with the objective of making a real mass balance between all the reagents and products at any time of the hydrogenolysis reaction, and this for various coverages of the metallic surface. For each experiment, 1 g of Pt/SiO_2 catalyst (corresponding to 24 μmol of Pt_s) and a given amount of Sn(*n*-$C_4H_9)_4$ (20 ± 2 μmol/g) were introduced into the reactor. In a given experiment, hydrogenolysis was allowed to continue for a given length of time, after which it was stopped. Reaction time was varied from 15 min to 50 h. Simultaneously, the evolution of *n*-butane was followed quantitatively by chromatographic analysis. After reaction the catalyst was washed to remove the unreacted tin complex which was also analyzed quantitatively. Chemical analysis of the catalyst was performed afterward to determine the percentage of tin grafted on the surface. The result of this set of experiments (Table 3) was a precise determination, at a given time of the reaction, of the average composition of the grafted organometallic $Pt_s[Sn(n\text{-}C_4H_9)_x]_y$.

From the data reported in Table 3, we can represent in Figure 5 the evolution of the average formula of the surface organotin species with the coverage. Careful examination of Figure 5 leads one to propose that the hydrogenolysis reaction of Sn(*n*-$C_4H_9)_4$ on the platinum surface is selective. After a short time

(49) Kunimori, K.; Uchijima, T.; Yamada, M.; Matsumoto, H.; Hattori, T.; Murakami, Y. *Appl. Catal.* **1982**, *4*, 67.

(50) Nédez, C.; Théolier, A.; Lefebvre, F.; Choplin, A.; Basset, J. M.; Joly, J. F. *J. Am. Chem. Soc.* **1993**, *115*, 722.

Table 3. Hydrogenolysis Reaction of Tetrabutyltin with Pt/SiO_2 (1 g) at 50 °C, Amount of Tin Fixed Obtained from the Difference between $Sn(n\text{-}C_4H_9)_4$ Introduced and Extracted (in parentheses is given the amount of tin fixed measured by elementary analysis), and Amount of Butane Evolved, Q_t

time (h)	$SnBu_{4\ introduced}$ (μmol/g)	$SnBu_{4\ extracted}$ (μmol/g)	Sn_{fixed} (μmol/g)	Sn/Pt_s	Q_t, C_4/Sn_{fixed}
0 h 15 min	18.6	14.7	3.9	0.14 (0.17)	1.0
0 h 30 min	20.0	13.5	6.5	0.23 (0.22)	1.2
1 h 2 min	19.7	11.6	8.1	0.29 (0.36)	1.6
2 h 2 min	20.8	9.6	10.4	0.37 (0.39)	2.0
5 h 10 min	20.6	8.5	12.1	0.43 (0.44)	2.3
10 h 16 min	21.1	5.9	15.2	0.54 (0.55)	2.6
25 h 40 min	21.1	3.4	17.7	0.63 (0.63)	3.0
39 h 40 min	21.1	0	21.1	0.75 (0.71)	3.0
50 h 0 min	20.0	0	20.0	0.71	3.0

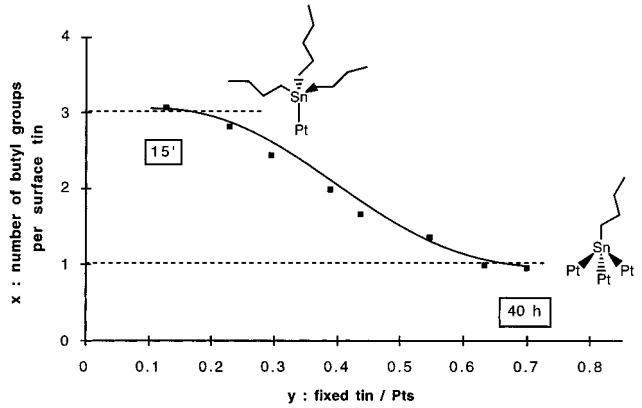

Figure 5. Reaction of $Sn(n\text{-}C_4H_9)_4$ on silica-supported platinum at 50 °C: evolution of the stoichiometry of surface organotin species with coverage.

of reaction, so at low tin loading, there is fast hydrogenolysis of one tin−carbon bond to form a $Sn(n\text{-}C_4H_9)_3$ surface fragment. Margitfalvi[51] has previously reported that the reaction of $Sn(C_2H_5)_4$ with alumina-supported platinum in benzene solution leads to a similar species. The extent of reaction was limited by the amount of irreversibly adsorbed hydrogen present. In our case, the reaction is performed without solvent and under hydrogen in excess. Then, successive hydrogenolysis of the two remaining butyl groups occurred up to the formation of a $Sn(n\text{-}C_4H_9)$ surface fragment which is stable even after 40 h of reaction.

To obtain an idea of the steric requirements of the surface organometallic fragments around the particle, it is interesting to plot the total number of butyl groups present on the surface (*xy*) and the amount of fixed tin (*y*), as a function of the reaction time. For coverages (Sn/Pt_s) greater than ca. 0.3, the *xy* value remains steady around 0.7 butyl groups per surface platinum atom (Figure 6). The number of butyl groups around the metal particule remains nearly constant whether the surface organometallic fragment is $Sn(n\text{-}C_4H_9)_3$, $Sn(n\text{-}C_4H_9)_2$, or $Sn(n\text{-}C_4H_9)$. This result suggests that the metallic surface is first rapidly covered by the $Sn(n\text{-}C_4H_9)_3$ fragments which apparently completely hinder the surface ($y < 0.3$). Then, it is necessary for these surface fragments to undergo a partial hydrogenolysis of Sn−C bonds before the incoming tetrabutyltin can react with the metallic surface.

This whole process seems therefore to be governed by this steric limitation.

(51) Margitfalvi, J.; Hegedüs, M.; Göbölös, S.; Kern-Tàlas, E.; Szedlacsek, P.; Szabö, S. In *Proc. Int. Congr. Catal., 9th* Weinheim: Berlin, **1984**, *4*, 903.

(52) Nédez, C.; Lefebvre, F.; Choplin, A.; Basset, J. M.; Benazzi, E. *J. Am. Chem. Soc.* **1994**, *116*, 3039.

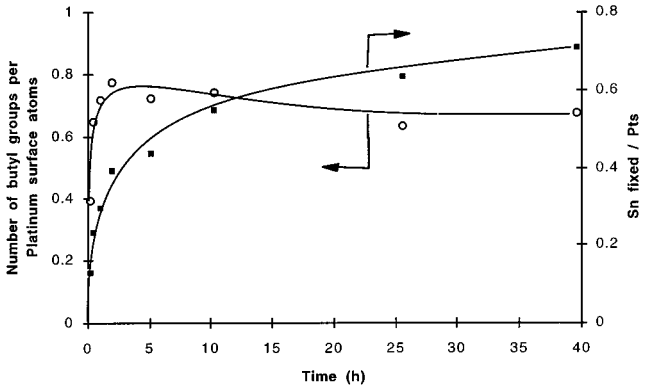

Figure 6. Reaction of $Sn(n\text{-}C_4H_9)_4$ on silica-supported platinum at 50 °C, evolution of the $Pt_s[Sn(n\text{-}C_4H_9)_x]_y$ species: total number of butyl groups per platinum surface atom (*xy*) and coverage of the surface Sn_{fixed}/Pt_s (*y*) as a function of time of reaction.

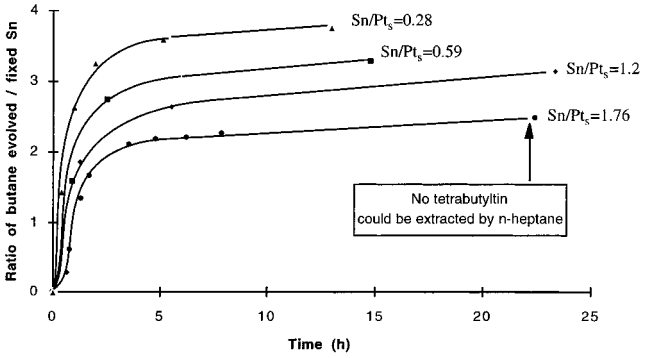

Figure 7. Amount of butane evolved during the reaction of $Sn(n\text{-}C_4H_9)_4$ on silica-supported platinum at 100 °C for various amounts of $Sn(n\text{-}C_4H_9)_4$ introduced.

At 100 °C, the surface reaction with Pt_s-H_x/SiO_2 is more complicated because the silanols of silica also react with the tetrabutyltin. This reaction has already been studied in detail.[50,52] In contrast to what is observed at 50 °C, even for ratios of $Sn(n\text{-}C_4H_9)_4$ introduced per surface platinum as high as 1.76, the totality of the $Sn(n\text{-}C_4H_9)_4$ is fixed (Table 2). The ratio of butane evolved by tin fixed with time and for various amounts of $Sn(n\text{-}C_4H_9)_4$ introduced is represented in Figure 7. At this temperature, the reaction of $Sn(n\text{-}C_4H_9)_4$ occurs both with the silica and the platinum surface, following eqs 1 and 2. The surface complexes $Pt_s[Sn(n\text{-}C_4H_9)_x]_y$ and $\equiv SiO-Sn(n\text{-}C_4H_9)_3$ are formed simultaneously. Note that the induction period observed is due to the time needed to reach 100 °C.

Although the surface reaction is complicated, it is nevertheless possible to determine the extent of the reaction occurring on the platinum by carrying out a blank experiment on pure silica with a given amount of $Sn(n\text{-}C_4H_9)_4$ (Figure 3). These experiments give the amount of butane evolved as a function of time and thus, according to eq 1, the amount of $\equiv SiO-Sn(n\text{-}C_4H_9)_3$ formed. The difference between the total amount of $Sn(n\text{-}C_4H_9)_4$ fixed and the amount of $Sn(n\text{-}C_4H_9)_4$ grafted only on SiO_2 gives the amount of $Sn(n\text{-}C_4H_9)_4$ fixed on the platinum surface (Figure 8).

The difference between the total amount of butane evolved at 100 °C in the presence of Pt/SiO_2 and the amount of butane evolved at the same time in the presence of SiO_2 gives us the amount of butane evolved according to eq 2. Figure 9 gives the number of butyl groups per fixed tin atom (*x*) on platinum as a function of time. There is first formation of a tri-*n*-butyltin surface complex which decomposes progressively with time to give $Sn(n\text{-}C_4H_9)$ and $Sn^{(0)}$.

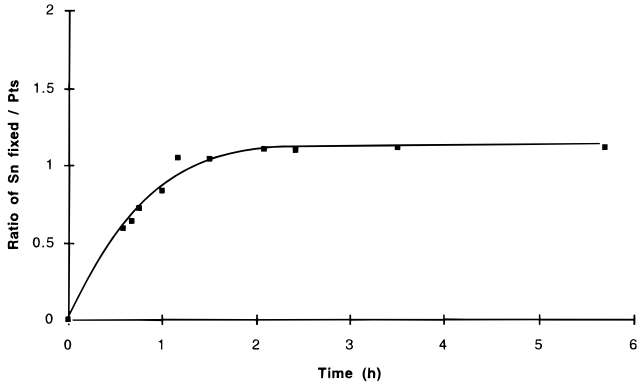

Figure 8. Reaction of $Sn(n\text{-}C_4H_9)_4$ (1.8 Sn_{int}/Pt_s) at 100 °C with Pt/SiO_2: evolution of tin covrage on platinum surface.

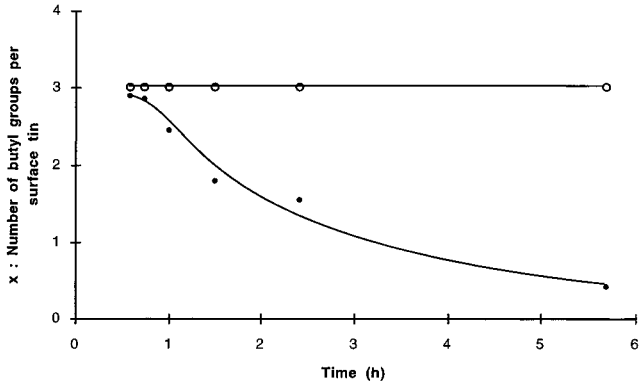

Figure 9. Hydrogenolysis reaction of $Sn(n\text{-}C_4H_9)_4$ (1.8 Sn_{int}/Pt_s) at 100 °C with Pt/SiO_2: evolution of the species grafted respectively on silica (○) and on platinum (◆).

Chart 1

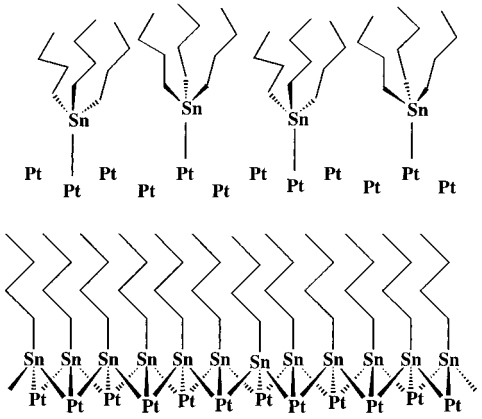

The Chart 1 represents the evolution with time of the surface compositon deduced from analytical data. At low coverage or for short reaction times, there is formation of a kind of close packing of $Sn(n\text{-}C_4H_9)_3$. It is only when some of these tributyl fragments are hydrogenolyzed that a new molecule of $Sn(n\text{-}C_4H_9)_4$ can react again with the surface of platinum to give a $Sn(n\text{-}C_4H_9)_3$ fragment.

3.2.2. Hydrogenolysis of the Grafted Complexes. The formation of a monobutyl species obtained at 50 °C (see Chart 1) is also clearly demonstrated by its hydrogenolysis at high temperature. It is possible to achieve the total hydrogenolysis of the grafted surface organometallic complex by treatment at 300 °C under hydrogen for 4 h. The last butyl group is fully hydrogenolyzed as butane. Traces amounts of propane, ethane, and methane are observed, but the main product is still butane.

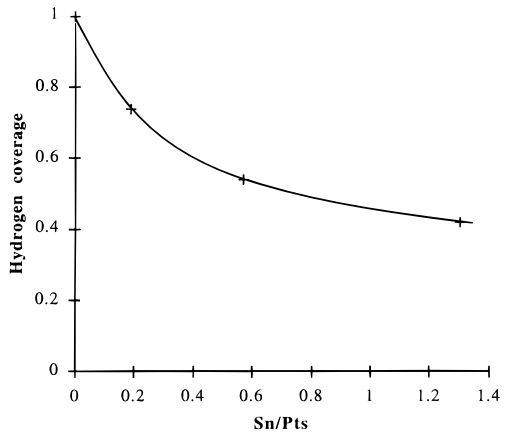

Figure 10. Coverage of the metalic particle $PtSn_y/SiO_2$ by chemisorbed hydrogen (25 °C and 150 mbar) with the amount of fixed tin (Sn/Pt_s).

The fact that there is no hydrogenolysis of the butane at 300 °C, even at low tin coverage, indicates that the tin atoms have already selectively poisoned the platinum surface.

3.3. Characterization of the $Pt-Sn/SiO_2$ Catalysts. 3.3.1. Electron Microscopy (CTEM and EDAX). These experiments were carried out on a sample which was prepared by hydrogenolysis of $Sn(n\text{-}C_4H_9)_4$ at 50 °C followed by a further treatment under hydrogen at 300 °C. Let us recall that such treatment leads to a selective reaction of the organometallic fragment on the platinum particule and not on the silica support. The size of the bimetallic particles ($Sn/Pt_s = 0.58$) measured by CTEM (Figure 2) was found to be greater than the size of the metallic particles of the corresponding monometallic starting material. On average, the diameter of the bimetallic particles increased by ca. 0.5 nm.

For the sample obtained by reaction of tetra-*n*-butyltin with Pt/SiO_2 at 100 °C followed by a treatment at 300 °C under hydrogen ($Sn/Pt_s = 1.8$), the increase of the size of the bimetallic particles was also ca. 0.5 nm. The result confirms that only a part of the tin introduced is present on the surface of the bimetallic particles and the other fraction must be bound on the silica surface. For this sample, the atomic ratio Sn/Pt measured by elementary analysis is ca. 0.8.

To determine where the tin is located namely on the particule or on the support, the electron beam was focused just on one metallic particle (9 nm^2) or on larger area (10^4 nm^2) which included both the metal particle and the support. The measured Sn/Pt ratios were respectively 0.55 ± 0.1 and 0.70 ± 0.1. The value obtained for larger zone ($Sn/Pt = 0.7$ in average) is consistent with the expected value from elementary analysis ($Sn/Pt = 0.8$), but the average ratio Sn/Pt on one metallic particle ($Sn/Pt = 0.55$) is lower than on larger area. This value is close to the ratio Pt_s/Pt computed with 2−3 nm particles (0.46−0.61). It appears that, as a first approximation, each surface platinum atom can accommodate a maximum of about one $Sn(n\text{-}C_4H_9)$ fragment which will undergo total hydrogenolysis on the metal surface and that the rest of the tetra-*n*-butytin will react with the silica surface.

3.3.2. Hydrogen Chemisorption. These experiments were carried out on Pt and Pt−Sn samples pretreated under hydrogen at 300 °C and then evacuated under vacuo (10^{-6} mbar) at the same temperature. The amount of hydrogen adsorbed at room temperature on the bimetallic catalyst is drastically lower than that adsorbed on a monometallic catalyst, presumably due to the presence of tin (Figure 10). These results are in agreement with previous ones obtained on similar bimetallic systems such

Table 4. Sn K-edge EXAFS-Derived Structural Parameters[a] for Supported Pt/Sn Species on Silica under Various Conditions

sample[b]	shell	coord no.	interatomic distance (Å)	$2\sigma^2$ (Å^2)[c]	*R* factor (%)
(i) 50 °C under H_2[e]	C	1.3(2)	2.12(1)	0.003(1)	37.6
	Pt	3.1(2)	2.716(9)	0.011(9)	
(ii) 300 °C under H_2[f]	Pt	4.2(2)	2.761(7)	0.0143(8)	39.1
(iii) 500 °C under H_2[g]	Pt	5.4(3)	2.784(9)	0.0156(9)	44.8

[a] NonFourier-filtered data. [b] For samples i−iii, EF = −12.1, −11.2, −12.4, and 14.4 eV, respectively, and AFAC = 0.88. [c] Debye−Waller factor. σ = root-mean-square internuclear separation. [d] *R* factor is defined as $(\int|\chi^\tau - \chi^E|k^3\,dk \int|\chi^E|k^3\,dk) \times 100\%$, where χ^τ and χ^E are theoretical and experimental EXAFS and *k* is the photoelectron wave vector. The values given in parentheses represent the statistical errors generated in EXCURVE; for details of true error estimation, see the Experimental Section. [e] Three-shell fit including the second carbon shell gave 1.0(2) Sn−C at 2.87(9) Å, with $2\sigma^2 = 0.04(5)$ Å^2, $E_f = -12.8$ eV, and *R* factor = 34.9%. [f] Two-shell fit including oxygen gave 0.5(2) Sn−O at 1.94(2) Å, with $2\sigma^2 = 0.015(6)$ Å^2, $E_f = -11.1$ eV, and *R* factor = 34.6%. [g] Two-shell fit including oxygen gave 0.2(2) Sn−O at 2.11(3) Å, with $2\sigma^2 = 0.009(5)$ Å^2, $E_f = -15.1$ eV, and *R* factor = 43.0%.

as Ru−Sn, Rh−Sn, or Ni−Sn.[20,23,25,26,28,53] The drastic decrease of H_2 adsorption is simply explained if one considers that in the bimetallic phase each element retains its chemical bulk properties: platinum metal is well-known to chemisorb hydrogen whereas tin metal does not.

Given this proposition, it may be surprising to observe that the amount of chemisorbed hydrogen is never zero. Let us consider that, during the hydrogenolysis of the tetra-*n*-butyltin with the platinum surface, a maximum of one organotin fragment could be grafted on each surface platinum atom. After treatment at 300 °C under hydrogen, the butyl groups are fully removed and the naked tin atoms are located on the surface of the bimetallic particle. The size of the bimetallic particle is greater than that of the monometallic particle (Figure 2), and thus, the number of surface atoms is also greater: Even for Sn/Pt_s equal to 1 in the starting material (after reaction at 50 °C), there are some uncovered platinum atoms on the surface of the bimetallic particle (after reaction at 300 °C).

For Sn/Pt_s ratios higher than unity, and for reaction temperatures higher than 100 °C, a fraction of the tin is located on the silica surface and, then, the coverage of the platinum surface remains constant and equal to unity.

3.3.3. EXAFS Studies of Silica-Supported Pt_x−Sn (*n*-C_4H_9) and Pt−Sn Surface Species. Sn K-edge EXAFS measurements (Table 4) were performed on three silica-supported Pt−Sn samples formed under a variety of conditions: sample i formed after partial hydrogenolysis of Sn(*n*-$C_4H_9)_4$ on Pt/SiO_2 at 50 °C under H_2; sample ii formed after further hydrogenolysis of sample i at 300 °C under H_2 (5 h); sample iii obtained after treating sample ii at 500 °C under H_2 (5 h). The objective of Sn K-edge EXAFS experiments was to provide direct information on whether the tin was attached to the platinum metal particles and/or to the silica surface and also whether the tin atoms were isolated from each other, which could be evidenced by the absence of Sn−Sn interactions.

The fitted k^3-weighted Sn K-edge EXAFS of sample i is shown in Figure 11a. The best fit to the k^3-weighted data was obtained with a model comprising ca. 1 C at 2.12 Å and 3 Pt at 2.72 Å (Table 4). The EXAFS-derived Sn−C distance is consistent with that expected for a tin−carbon σ-bond, and the Sn−Pt distance of 2.72 Å falls within the range (2.5−2.8 Å) previously reported in the literature.[29,30,54−57] Any attempt to include Sn−O or Sn−Sn interactions resulted in significantly higher *R* factors, suggesting that the tin atoms are isolated and bonded directly to Pt rather than to the silica surface. To further investigate the feasibility of a $Sn-O_{surface}$ contribution to the EXAFS, refinements were also carried out using k^1-weighting since such a weighting favors near shells of light scatters (O and C backscattering decays rapidly with increasing *k* value) whereas k^3 emphasises the higher shells. In addition, the backscattering functions of Pt and Sn are significantly different at low *k* values, so distinction between these two elements should be aided (even when both coordination distances are the same). The k^1-weighted Sn K-edge EXAFS of sample i, fitted with analogous C and Pt shells as for the k^3-weighted data, is given in Figure 11b. The k^1-weighted Sn K-edge EXAFS-derived parameters (1.1 C at 2.12 Å; 3.0 Pt at 2.72 Å) agree very nicely with those obtained from the k^3 fit (1.3 C at 2.12 Å; 3.1 Pt at 2.72 Å). Additional Sn−O interactions at ca. 2 Å could not be modeled satisfactorily to the EXAFS, and any attempt to replace the C shell at 2.12 Å by O resulted in a significantly higher *R* factor. Nor could any evidence for Sn−Sn interactions could be found. A slight improvement was noted however when a C shell at 2.87 Å was included in the refinement (Figure 11c). Such a shell could be accounted for by the β-C of the butyl, lending further support to the presence of this ligand. If one assumes a C−C distance of 1.54 Å, a Sn−C distance of 2.11 Å, and a Sn−C−C angle of 109°, the $Sn\cdots C_\beta$ distance would be expected at 2.99 Å; the EXAFS-derived distance of 2.87 Å is somewhat shorter than expected. Given the quality of the data and the fact that the drop in *R* factor is less than 10%, it is however hard to justify the inclusion of this shell much further in the discussion. In summary then, the Sn-K edge EXAFS of sample i appears to be consistent with one butyl ligand remaining on tin at 50 °C and that tin is bonded directly to three platinum atoms. There is no evidence from the EXAFS analysis to suggest that the butyl species are linked to the silica surface via σ-bonded ≡SiO− groups, nor is this particularly likely since control reactions of Sn(*n*-$C_4H_9)_4$ introduced onto silica at 50 °C in the absence of platinum have demonstrated that the reaction between Sn(*n*-$C_4H_9)_4$ and silica is negligible at this temperature (see section 3.2.1). The Sn K-edge EXAFS results are thus consistent with the analytical data resulting from the hydrogenolysis experiments, and they support the formation of monobutyltin species i (Chart 2) on the platinum surface at 50 °C.

On heating of sample i to 300 °C in the presence of hydrogen (sample ii), a significant change in the Sn K-edge EXAFS was observed. Initially, a satisfactory fit was produced by modeling the k^3-weighted data with a single shell of ca. 4 Pt atoms at 2.76 Å (Figure 12a, Table 4), indicating a loss of butyl ligands. The coordination number of 4 Sn−Pt is comparable to that found by Iwasawa[29] for Pt−Sn/SiO_2 catalysts prepared from $Sn(CH_3)_4$. Additional Sn−Sn interactions at ca. 2.6 Å were also reported by Iwasawa, and indeed, refitting our Sn K-edge EXAFS in k^1-weighting (Figure 12b) revealed a much poorer match at low *k*, suggesting that there might be a Sn contribution. However, attempts to model a shell of Sn at ca. 2.6 Å to the k^1-weighted data produced no improvement in the *R* factor. Inclusion of 0.5 O at 1.94 Å, on the other hand, did give a significant

(53) Coq, B.; Goursot, A.; Tazi, T.; Figuéras, F.; Salahub, D. *J. Am. Chem. Soc.* **1991**, *113*, 1485.
(54) Holt, M. S.; Wilson, W. L.; Nelson, J. H. *Chem. Rev.* **1989**, *11*, 89.
(55) Uson, R.; Fornies, J.; Tomas, M.; Uson, I. *Angew. Chem., Int. Ed. Engl.* **1990**, *29*, 1449.
(56) Almenningen, A.; Haaland, A.; Wahl, K. *J. Chem. Soc., Chem. Commun.* **1968**, 1027.
(57) Lindsey, R.; Parshall, G. W.; Stolberg, U. G. *Inorg. Chem.* **1966**, *5*, 109.

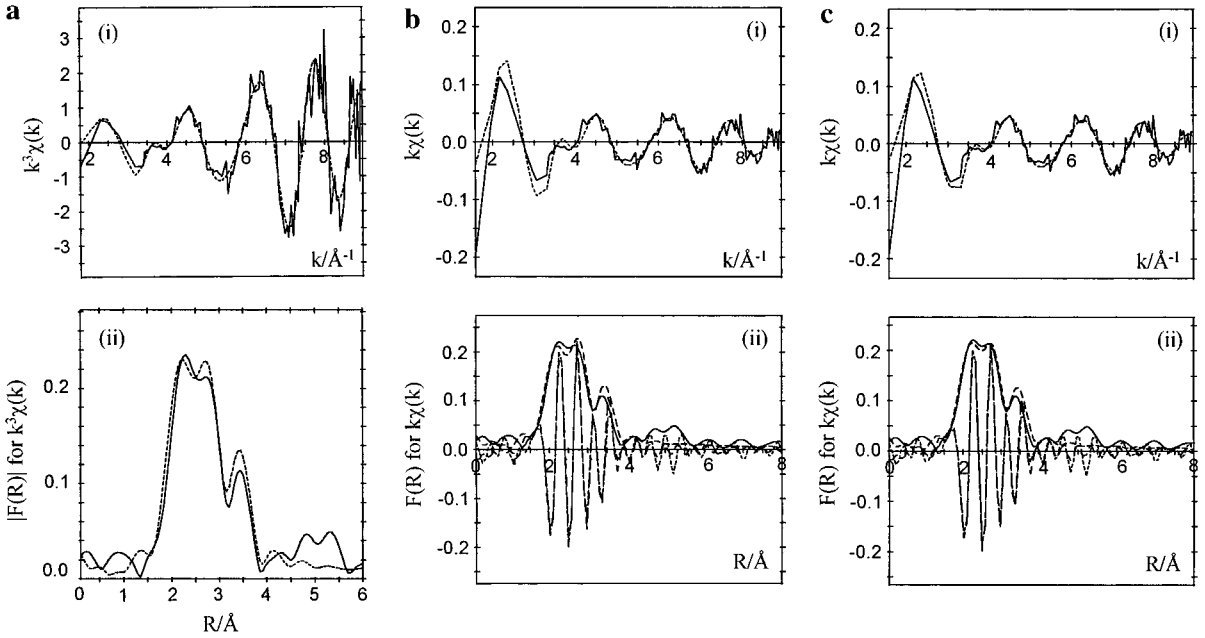

Figure 11. Sn K-edge k^3-weighted EXAFS (i) and Fourier transform (ii), phase-shift corrected for carbon, of Pt−Sn/SiO_2 species formed at 50 °C under H_2 (—) experiment and (- - -) spherical wave theory.

Chart 2

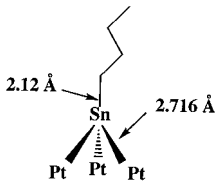

reduction in *R* factor (Figure 13c). Such a shell could be accommodated by the migration of a small amount of Sn to the silica surface. However, since the oxygen contribution was found to vary widely according to the background substraction used, the validity of this shell must be regarded with some suspicion. The Pt L_{III}-edge EXAFS of sample ii was also recorded in the hope that Pt−Sn interactions might be identified in addition to Pt−Pt. Again, both k^1- and k^3-weighted refinements were carried out but neither showed any conclusive evidence for the presence of Sn as backscatterer, fitting instead to a single shell of ca. 9 Pt at 2.7 Å. This is perhaps not too surprising if one considers the total number of Pt−Pt versus Pt−Sn interactions in, for example, a 26 Å diameter cubo-octahedral platinum particle (see Table 1). Such a particle would contain a total of 586 atoms, of which 272 are surface platinums and the average Pt coordination number[58,59] would be on the order of 9−10. Thus, the Pt−Sn contribution to the EXAFS (assuming 1 Sn bound to 1 Pt_s) would be 5% at maximum and would decrease rapidly with increasing particle size and with lower Sn/Pt_s ratios. Even allowing for some penetration of Sn into the surface Pt layer, it would be hard to justify the inclusion of Pt−Sn interactions in the Pt L_{III}-edge EXAFS given the size of the particles. Our results are also consistent with the Pt L_{III}-edge EXAFS reported by Iwasawa[29] where only Pt atoms (ca. 7−8 at 2.77 Å) were identified in the first coordination shell and no Pt−Sn interaction were observed.

Further heating of the Pt−Sn/SiO_2 species ii to 500 °C under hydrogen caused no significant change in the Sn K-edge EXAFS, with the k^3-weighted data (Figure 13a) being best modeled by single Pt shell of *ca.* 5 atoms at 2.75 Å (Table 4). Analysis of the k^1-weighted EXAFS with the single-shell model again gave a poor fit at low *k* (Figure 13b), but in this case, an additional shell of 0.2 O at 2.11 Å (Figure 13c) failed to produce a stable refinement and no significant drop in *R* factor resulted, nor were any Sn−Sn interactions evident. Since the EXAFS-derived Sn−Pt coordination numbers for the samples treated at 300 and 500 °C are much lower than expected for the given particle size (from TEM), our results would suggest that the Sn atoms are located close to the external surface of the platinum metal particles rather than in the bulk. The increase in the Pt coordination numbers from initially 3, to ca. 4 then 5 on heating from 300 to 500 °C could be interpreted as penetration of Sn deep inside the Pt metal particles. Also, while it cannot entirely be ruled out that a small percentage of Sn has migrated to the silica surface on heating the Pt−Sn/SiO_2 species, the absence of Sn−Sn interactions in the EXAFS does suggest that the Sn atoms remain essentially isolated on the particles.

3.3.4. Molecular Modeling. We have suggested in section 3.2.1. that the hydrogenolysis of Sn(n-C_4H_9)$_4$ on the platinum surface at 50 °C is governed by steric limitations due to the bulkiness of the butyl ligands or more precisely the "cone angle" of the grafted tin (alkyl(s)). When the tin coverage of the platinum surface is low, that is less than 0.3 Sn/Pt_s, it has been demonstrated that the surface organometallic fragment Sn(n-C_4H_9)$_3$ is the only species formed. At higher coverage of the metallic surface, and for long reaction periods, a Sn(n-C_4H_9) fragment is stable. In any case, no more than 0.7 butyl groups per surface platinum atom can be observed at any Sn/Pt_s coverage. Everything occurs as if there was a kind of "close packing" of surface alkyls fragments, regardless of the coverage of the surface by tin atoms.

It was therefore interesting to model the surface organometallic species formed on a platinum particle of 201 atoms with a cubo-octahedral shape ($Pt_s = 122$, $D = 0.60$). This could be achieved by grafting increasing amounts of −Sn(n-C_4H_9) fragments. The overall energy of the system, measured for respectively 72, 96, and 120 fragments is reported in Figure 14.

(58) Benfield, R. E. *J. Chem. Soc., Faraday Trans.* **1992,** *88*, 1107.
(59) Kip, B. J.; Duivenvoorden, F. B. M.; Koningsberger, D. C.; R., P. *J. Catal.* **1987**, *105*, 26.

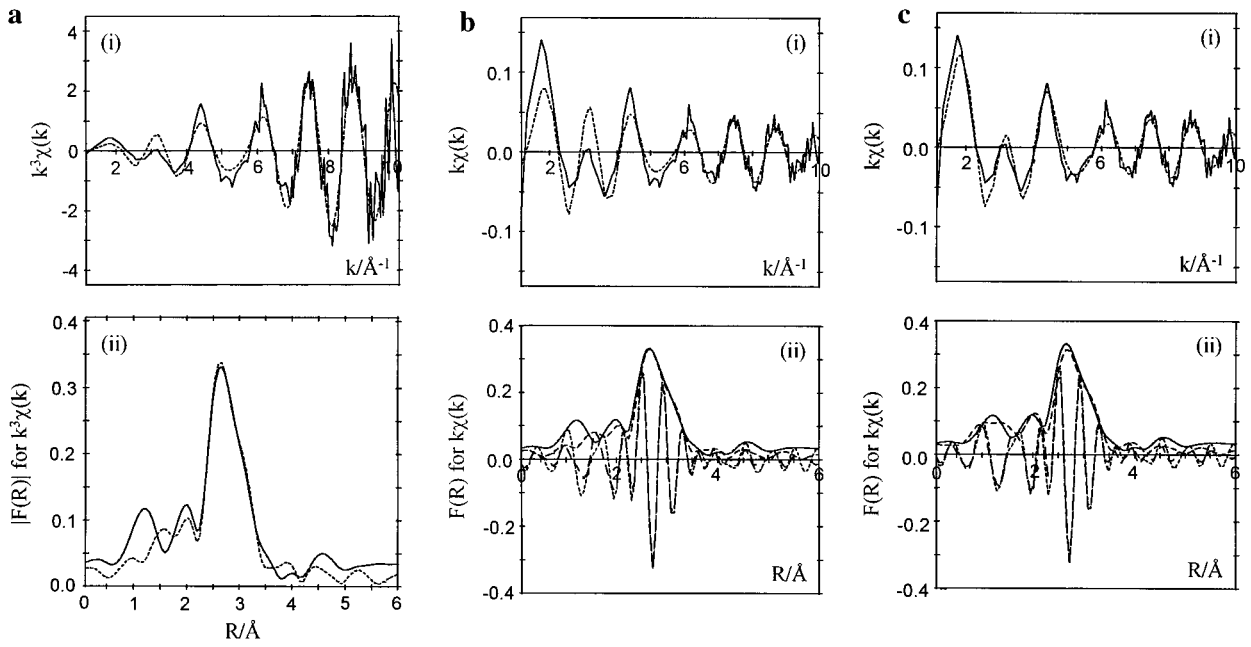

Figure 12. Sn K-edge k^3-weighted EXAFS (i) and Fourier transform (ii), phase-shift corrected for platinum, of Pt−Sn/SiO_2 species formed at 300 °C under H_2 (—) experiment and (- - -) spherical wave theory.

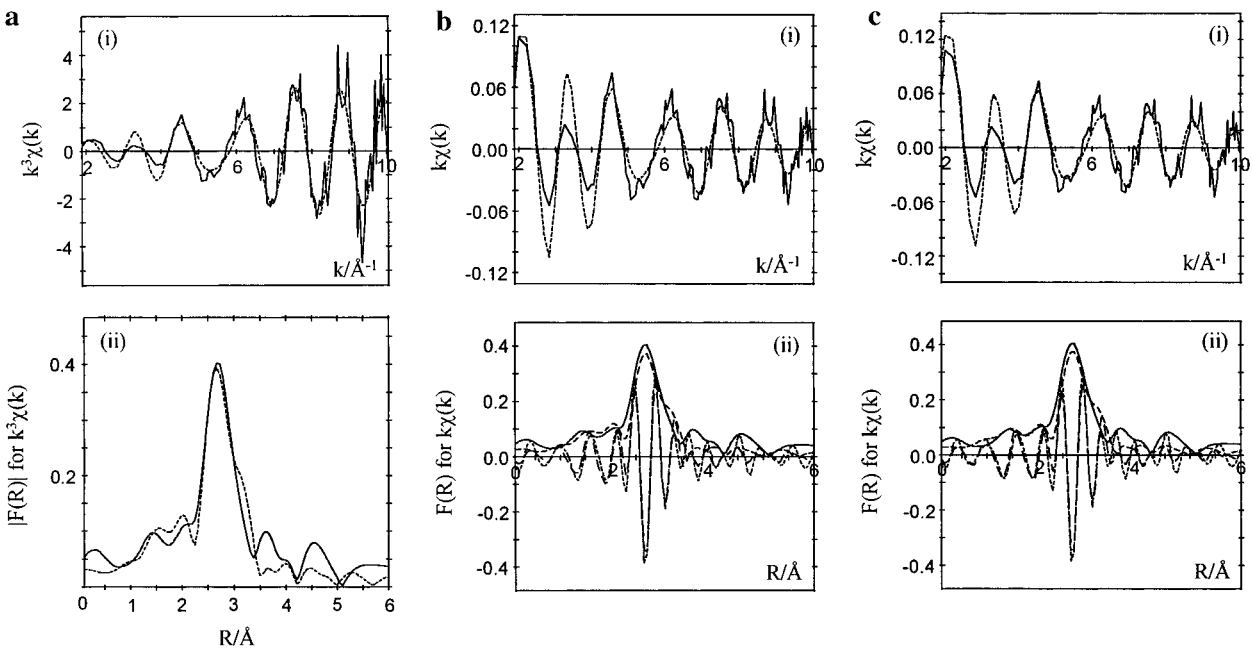

Figure 13. Sn K-edge k^3-weighted EXAFS (i) and Fourier transform (ii), phase-shift corrected for platinum, of Pt−Sn/SiO_2 species formed at 500 °C under H_2 (—) experiment and (- - -) spherical wave theory.

The resulting energy is minimum for 96 grafted fragments which corresponds to a Sn(n-C_4H_9)/Pt_s ratio of 0.78. In this case, due to Van der Waals interactions between the chains, like in Langmuir−Blodgett layers, the energy is lower than with 72 fragments. For 120 grafted fragments, which corresponds to a surface coverage of unity, the steric repulsion increases drastically due to van der Waals repulsions and the total energy reaches more than 2 kcal/C, which obviously prohibits such a situation.

To summarize, the grafting of SnBu fragments on a particle of 200 atoms reaches a minimum of energy for a platinum coverage of 0.78 in fairly good agreement with the experimental results. This situation is not very different from that already observed for carbonyl clusters of high nuclearity, where the number of carbonyl ligands around the cluster framework is governed by their steric requirements rather that by the number of metallic atoms at the periphery of the cluster (see for example the cluster $[Pt_{38}(CO)_{44}]^{2-}$).[60]

4. Conclusion

The selective hydrogenolysis of Sn(n-C_4H_9)$_4$ on silica-supported platinum is a stepwise process which leads to various kinds of surface tri-, di-, and monobutyl fragments which undergo complete hydrogenolysis to tin "adatoms" which are further incorporated into the particle.

At 50 °C and under 30 mbar of hydrogen, Sn(n-C_4H_9)$_4$ reacts selectively with the platinum surface with formation of *n*-butane

(60) LCOMS databank: URL: http://www.univ-lyon1.fr/fb/lcoms/datacryst.htlm.

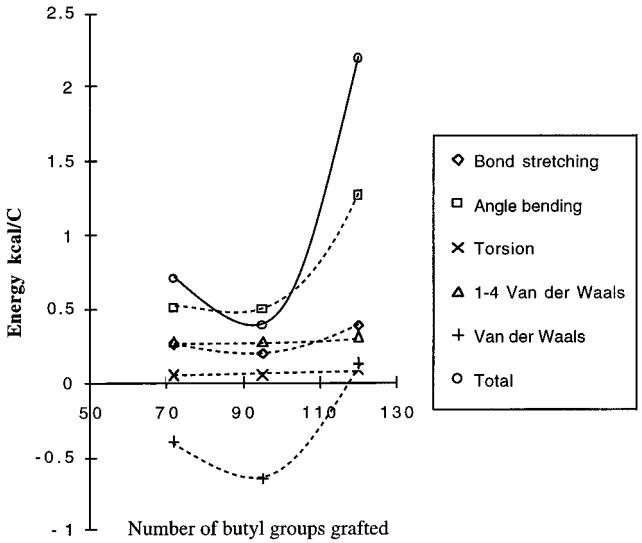

Figure 14. Energy of the system, measured for respectively 72, 96, and 120 $Pt_s-[Sn(n\text{-}C_4H_9)]$ fragments.

and a grafted species which could be described as $Pt_s[Sn(n\text{-}C_4H_9)_x]_y$. The value of y (Sn/Pt_s) is never higher than unity even when the amount of $Sn(n\text{-}C_4H_9)_4$ introduced by Pt_s is higher than unity. This corresponds to the typical behavior of a surface reaction rather than a bulk reaction. The rate of the reaction is low, since more than 40 h is needed to reach a kind of equilibrium. The reaction begins by the hydrogenolysis of one butyl group, with formation of a $Pt_s-Sn(n\text{-}C_4H_9)_3$ fragment. Due to steric hindrance of the $-Sn(n\text{-}C_4H_9)_3$ fragment, the coverage of the platinum surface is no more than ca. 0.2 tin centers per surface platinum atom. This species is not stable with respect to further hydrogenolysis. This hydrogenolysis of the grafted tin tributyl gives a tin dibutyl which results in a decreased steric hindrance and an increase of the surface coverage. During this reaction, the total number of butyl groups which are present on the surface remains constant and close to 0.8. At 50 °C, a stable situation is reached where only one butyl group per tin atom remains on the surface. This stable surface organometallic compound has the following formula: $(Pt_s)_3[Sn(n\text{-}C_4H_9)]$. The presence of this species is confirmed by EXAFS analysis (Chart 2). Further increase of the temperature to 300 °C leads to complete hydrogenolysis into tin adatoms. At 500 °C, tin migrates into the particule sublayers.

At 100 °C and under 30 mbar of hydrogen, $Sn(n\text{-}C_4H_9)_4$ reacts simultaneously with the platinum and the silica surfaces with formation of grafted species and *n*-butane evolution. The formed species could be described by $Pt_s[Sn(n\text{-}C_4H_9)_x]_y$ and $\equiv SiO\text{-}Sn(n\text{-}C_4H_9)_3$. The latter one however was previously described and well characterized by Nédez.[50] The rate of $Sn(n\text{-}C_4H_9)_4$ reaction with silica alone is very low as compared with the rate of reaction with the Pt/SiO_2 catalyst; only 1 h is needed to completely cover the platinum surface, and 24 h is needed to graft the same amount of $Sn(n\text{-}C_4H_9)_4$ on the silica surface. The amount of $Sn(n\text{-}C_4H_9)_4$ which reacts with the platinum surface ($y = Sn/Pt_s$) is never greater than 1, even when the amount of $Sn(n\text{-}C_4H_9)_4$ introduced by Pt_s is higher than unity. The reaction of $Sn(n\text{-}C_4H_9)_4$ with Pt_s begins with the formation of the $Pt_s[Sn(n\text{-}C_4H_9)_3]$ species which is not stable and undergoes almost complete hydrogenolysis after 6 h of reaction.

The two species which are formed, on the silica or on the platinum surface, can be completly dealkylated when they are treated under hydrogen at 300 °C. The bimetallic material obtained adsorbs less hydrogen than the starting monometallic catalyst.

JA964405O